Hydraulic Fracture Plan PNR 2

Management System:	HSE	**File Name:**	CORP-HSE-RPT-003
Approver:	Technical Director: Signed:	**Version No:**	3.0
Reviewer:	Frac Manager, Senior Geoscientist, Project Director	**Date of Issue:**	July 2019
Author:	Geophysicist, EPP Manager	**Proposed date of Review:**	n/a

Version	Section	Revision Information	Date	Reviser
0.1	All	Draft Publication	Jul 17	Senior Geoscientist
0.2	All	Update to document post drilling PNR2	Aug 18	HSE&P Manager | Geophysicist
0.3	All	Update after review	May 2019	EPP Manager | Geophysicist
1.0	All	Submitted version	May 2019	EPP Manager | Geophysicist
2.0	All	Submitted version	June 2019	EPP Manager | Geophysicist
3.0	All	Updated text in accordance with Tracker and App 6	July 2019	EPP Manager | Geophysicist

Documents are reviewed as per proposed review date, or sooner if a significant change to the operation has taken place, to ensure relevance to the systems and process that they define.

Contents

1.0 Well Classification

Well Name:	**Preston New Road-2**
Operator:	Cuadrilla Bowland Ltd
License:	EXL269 (for site location), PEDL165 (for lateral well)
Partners:	PEDL165 Cuadrilla Resources Ltd – 51.25% Spirit Energy- 25% AJ Lucas – 23.75%
	EXL269 Cuadrilla Resources Ltd – 53.5%; Spirit Energy – 22.75%, AJ Lucas 23.75%
Lateral Length MD	745 m
Lateral Depth TVD	2100-2116 m
Surface Coordinates:	Northing 432752.17 m Easting 337437.77 m [BNG - OSGB36]
	Lat 53° 47’ 14.3712" N Long 02° 57’ 03.7984" W [WGS84]
TD Coordinates:	Northing 432718.02 m Easting 335792.01m [BNG - OSGB36]
	Lat 2° 58’ 33.6850" W Long 53° 47’ 12.5435" N [WGS84]

a Introduction

During 2018, hydraulic stimulation of 17 stages on PNR1z tested the assumptions and effectiveness of the procedures detailed within this Hydraulic Fracture Plan (HFP). The procedures set out within this HFP (PNR2), such as the use of a traffic light system to mitigate seismicity, are not significantly adjusted from the 2018 HFP (PNR1z) as operations were executed safely within these procedures, as expected. Minor adjustments post learnings are detailed below;

Update	**Relevant section(s)**
Addition of two small scale features observed in Microseismic data	j Microseismic Geological Features Appendix 1: Lower Bowland Depth Structure Map Appendix 2: x Geological Cross Section PNR2
Extended interpretation of SD5	h Seismic Discontinuities Appendix 1: Lower Bowland Depth Structure Map
Development of reporting requirements	6.0 Reporting
Update to fracture modelling to include higher viscosity frac fluid	Appendix 5: Fracture Model Graphical Representation
Improved GMPE	Appendix 6: Ground Motion Prediction Equation (GMPE

2.0 Faulting

b Local Faulting

Name	Type	Distance to nearest injection point m	Dip	Strike	Throw m	Slip Tendency	Coulomb Stress Change	Sleeve	S_H [ºN]
Moor Hey	Reverse	1450	53□E	041□	730	0.48	0.0014MPa	47	045□
Anna's Road	Reverse	800	40□E	061□	650	0.87	0.0051MPa	47	145□
Haves Ho	Reverse	1500	50□E	044□	1700	0.54	0.0022MPa	47	060□
PNR-1	Reverse	550	60□E	019□	200	0.80	0.0192MPa	47	045□
Fault-2	Reverse	1300	85□E	032□	30	0.52	0.0160MPa	44	025□
Thistleton	Normal	2000	68□E	030□	850	0.90	0.0007MPa	47	060□

c Fault Reactivation

Fault reactivation is split into two assessments, risk to groundwater/permit boundary compliance and risk of induced seismicity. Respectively, the Environment Agency (EA) assess the risk to groundwater/permit boundary compliance and the Oil and Gas Authority (OGA) assess the risk of induced seismicity.

d Groundwater/ Permit Boundary Compliance

The possibility of hydraulic fracturing causing fault reactivation leading to a pathway from the Bowland Shale towards and intersecting a groundwater bearing unit has been previously assessed within the PNR Environmental Statement (ES), chapter 11 Hydrogeology and Ground Gas(17). While hydraulic fractures could potentially intersect existing faults at depth within the shale, there is a very low likelihood of S-P-R (Source, Pathway, Receptor) linkage for fracturing fluid propagating outside the permitted boundary to a groundwater bearing unit. This is due to the short-lived pressures associated with hydraulic fracturing not enabling an upward migration of fluids over a significant distance and the contrast in geomechanical properties between the Upper Bowland Shale and the overlying Millstone Grit. At the Preston New Road Site, the Millstone Grit overlies the Upper Bowland Shale. Observations in section v "Well Observation" identify the Millstone Grit to be absent at the PNR1 well pilot hole location, however 3D seismic data suggests the presence of the Millstone Grit vertically above the lateral well (PNR2). The lateral well PNR2 is drilled towards the base of the Upper Bowland shale with 200m of Upper Bowland present above the well providing a barrier between this well and the upper permit boundary. Consequently the assessment of the risk has not altered the conclusions reached in the Environmental Statement (ES) and the associated mitigation measures remain consistent with the previous ES assessment. Furthermore the distances noted in section b "Local Faulting" and section h "Seismic Discontinuities" have been verified and updated on analysis of the lateral wellbore PNR2. Consequently a direct discharge of fracturing fluid into the Millstone Grit remains a very low likelihood based on this updated assessment.

Critically stressed faults have been remodeled in accordance with the commitment made in the Environmental Statement "the stress orientation and magnitude will be measured in the vertical pilot hole and will form the basis of the stress information used in the HFP". The conclusion of the remodeled critically stressed faults are assessed in section f "Slip Tendency Analysis".

A progressive stepped approach will be adopted during the hydraulic fracturing operation, e.g. using mini-fractures and previous fracture stage information, to verify that the risk remains very low. Detailed fracture modelling to assess this risk is described in section 4.m "Fracture Modelling". The modelling performed demonstrates that in no single case does fracturing fluid migrate outside the permitted boundary. This assessment has been verified by microseismic monitoring observations of injection stages performed on PNR1z. As demonstrated in the submitted daily reports, no fracture growth was observed beyond the permitted boundary. The risk remains very low for fractures to extend beyond the permitted boundary.

e Induced Seismicity

Cuadrilla is anticipating that the horizontal well bore, or the area intended to be hydraulically stimulated, will encounter a number of small local faults(8) within the shale rock. For the purpose of this assessment it is assumed that all faults within the area are 'critically stressed'. As observed during fracturing operations along PNR1z, two additional geological features were identified and are detailed in section i "Microseismic Geological Features". This is a conservative assumption as in reality not all faults will be critically stressed. Modelling a conservative assumption (direct injection into a predicted or unpredicted critically stressed fault) and using 2000 m^3 injection stages the upper bound estimate for the maximum induced seismic event magnitude possible, in the absence of any mitigating measures, would be 3.1 M_L(7). The likelihood of this upper bound event occurring is considered to be very low(9). Induced seismicity along PNR1z has been significantly lower than this upper bound estimate with the largest event to date being 1.5 ML. As the geomechanical inputs to this maximum magnitude calculation have not changed, the assumptions and conclusions of the modelling are still relevant and have not been updated. The assumptions of the model will be updated as detailed in section 7.0 "Verifications Updates" of this plan and continued to be adapted during the hydraulic fracturing phase, by utilizing information from mini-fractures and previous fracture stages, to inform the decision tree in Appendix 4. Furthermore the embedded mitigation outlined in Chapter 12 of the Environmental Statement will significantly reduce the risk of induced seismic events occurring.

f Slip Tendency Analysis

The data collected through extended leak-off tests and image logging in the PNR1 and PNR1z wells allowed for a re-interpretation of the stress field. Stress gradients at reservoir level (at approximately 2,200 m depth) are as follows:

Shmin = 14 ppg = 0.0164 MPa/m

SHmax = 27 ppg = 0.0317 MPa/m

Sv = 21.5 ppg = 0.0252 MPa/m

Pore pressure = 11.23 ppg = 0.0132 MPa/m

During fracturing operations of PNR1z observed Sh min values lie between 0.0148 MPa/m and 0.0197 MPa/m, as such the Sh min used within the slip tendency analysis is still considered appropriate. The empirical evidence derived by microseismic observations of activated geological structures confirms that unidentified critically stressed local faults are present and are likely to slip. Subsequently a model update will not change existing mitigation measures, or provide additional assurance as this modelling is superseded by the microseismic observations used to identify them and the learnings that direct injection of these features causes low level seismicity. As such slip tendency modelling included here will not be re-performed.

The orientation of SH max rotates with depth. At reservoir level an orientation of 141° N is used. Using these geomechanical inputs, slip tendencies have been calculated for local faulting and seismic discontinuities. The interpretation of absolute ST values is not straightforward since the strength of faults is generally unknown. With the simplifying assumptions of a regional stress field without lateral variations and no variations of fault strength, ST values can be interpreted in a relative sense, i.e. faults with the largest ST values are interpreted as potentially being critically stressed, whereas those faults exhibiting smaller ST values are considered to be stable. Analysis for the nearby Preese Hall (PH_Max) fault, which has been seismically activated, gives a maximum slip tendency of ST=0.78 for this fault.

Comparing absolute ST values to the slip tendency obtained for the Preese Hall fault, the following faults (Section b) and Seismic Discontinuities (Section h) are considered as (potentially) being critically stressed (see Appendix 1: Lower Bowland Depth Structure Map for locations):

- SD3
- Thistleton fault
- Anna’s Road fault
- PNR-1 fault
- SD5
- SD6

Additionally, SD1 and SD4 exhibit slip tendency values ≥ 0.7 corresponding to near-critical stress conditions when compared to the Preese Hall fault. The stress impact of the fracturing operations on the slip tendencies is calculated while systematically varying the orientation of SH max between 25°N to 145°N in steps of 5°. The slip tendencies provided in this document are the worst case result from this SH max variation. A significant increase of the ST value is obtained for the SD3 fault only. These can be addressed with the extreme case simulations outlined in section e Induced seismicity. During hydraulic fracturing operations at PNR1z, the following faults; Thistleton, Anna’s Road, PNR-1, SD3 and SD6 showed no activation. SD5 did show microseismic activity confirming it to be a true geological structure, however this did not lead to activity beyond the permit boundary, or any adverse seismicity.

g Coulomb Stress Change Analysis

Coulomb stress changes (DCS) associated with the planned hydraulic fracturing operations have been numerically simulated. For each fracturing stage, cumulative stress contributions from all previous stages were considered. Fracture models were simulated with a frack opening width of 40 mm(3). These simulations are repeated accounting for the modified stage locations and the refined fault trajectories. Orientation of SH max which is varied between 25°N to 145°N in steps of 5°. The resulting maximum DCS values per fault and fracturing stage are presented within the fault and seismic discontinuities tables as the worst case result. The level of 0.1 MPa is considered to be a lower limit below which demonstrate that triggering of seismic events is considered unlikely. Simulated Coulomb stress changes (DCS) are presented for each fault and fracturing stage separately. For each fracturing stage, a single DCS value is provided, which refers to the 10 m x 10 m fault patch with the largest DCS. In all cases, the maximum DCS value is provided in the figure title together with the associated stage number and stress field orientation.

h Seismic Discontinuities

Name	Type	Distance to nearest injection point m	Dip	Strike	Throw m	Slip Tendency	Coulomb Stress Change	Sleeve	S_H [ºN]
SD1	Reverse	750	53□E	021□	30	0.70	0.0045MPa	47	085□
SD2	Reverse	700	73□E	070□	40	0.65	0.0171MPa	47	040□
SD3	Normal	300	75□E	150□	25	0.96	0.1218MPa	47	135□
SD4	Reverse	450	42□E	033□	25	0.76	0.0322MPa	47	045□
SD5	Reverse	200	50□E	022□	20	0.79	0.0505MPa	01	050□
SD6	Normal	800	67□E	030□	60	0.79	0.0202MPa	47	075□

Note: Although the SD3 feature is laterally adjacent it has not been observed in the PNR2 or PNR1z (HFP PNR1z$_{(18)}$) wellbores.

The nearest seismic expression of SD3 is 300m from the nearest injection point. The model predicted a larger DCS, only marginally above the 0.1MPa, due to the proximity of this feature. This is modelled as a worst case scenario where no embedded mitigation measures are employed. However in practice the real time microseismic array will be used to monitor fracture growth relative to the SD3 feature. If microseismic data indicates direct injection into the SD3, and that the SD3 feature is interpreted to be a fault, then pumping operations will be modified to reduce the likelihood of further connectivity with SD3. Microseismic observations of SD5 indicate the nearest seismic expression of SD5 is now 200m from the nearest injection point along PNR2, previously 400m. Slip tendency modelling of the adjusted SD5 will not change existing mitigation measures, or provide additional assurance. This modelling is superseded by the microseismic observations used to identify SD5, showing that direct injection into this feature causes low level seismicity. Therefore slip tendency modelling will not be re-performed.

i PNR2 Wellbore Identified Faults / Soft Sedimentary Structures

Name	Type	Distance along Wellbore MDRT	Dip	Strike	Throw m	Slip Tendency	Coulomb Stress Change	Sleeve	S_H [ºN]
1	N/A	2418	N/A	N/A	N/A	N/A	N/A	47	N/A
2	N/A	2557	N/A	N/A	N/A	N/A	N/A	39	N/A
3	N/A	2973	N/A	N/A	N/A	N/A	N/A	10	N/A

Note: Wellbore Identified features in the horizontal section of PNR2

During drilling of the PNR2 well, three minor but identifiable structural changes were observed in the lateral section. Structural changes 1 and 2 were identified using a resistivity imaging tool, change 3 was identified using an azimuthal gamma tool that allows bedding dip to be estimated. It cannot be conclusively determined whether these structural changes shown by bedding dip changes are a result of soft sedimentary deformation, which is frequently observed in the PNR1 pilot well core or small scale faults. These structures intersected were too small to be resolved in the 3D seismic data. Orientation and extension of these structures are only loosely constrained by the depth in which they were observed. Therefore, these structures are not included in the specific sensitivity analysis due to the lack of analytical description available and instead are addressed with the extreme case simulations outlined in section e Induced seismicity. The structures are located between the fracturing stages and will most likely be intersected by a hydraulic fracture. However given the small dimension of these structures it is considered very unlikely that these structures could respond with noticeable induced seismicity.

j Microseismic Geological Features

Name	Type	Distance to nearest injection point m	Dip	Strike	Throw m	Slip Tendency	Coulomb Stress Change	Sleeve	S_H [ºN]
MSPNR1z_i	N/A	0	90□E	165□	<40	N/A	N/A	N/A	N/A
MSPNR1z_ii	N/A	0	85□E	050□	<40	N/A	N/A	N/A	N/A

During Hydraulic Stimulations of PNR1z, two additional features were identified through the interpretation of Microseismic data, the closest associated event is 100m laterally and 60m below PNR2 proposed operations. These features cannot be seen to extend to the PNR2 wellbore in the current dataset, however additional unidentified critically stressed local faults are likely to be present. Induced seismicity from these features is mitigated by the same operational procedures set out in this HFP.

k Fault Criticality Conclusions

This sensitivity analysis indicates that Coulomb stress changes due to the fracturing operations are in general extremely small (i.e. < 0.1 MPa), in particular all significant faults which can clearly be identified in seismic sections. Greater Coulomb stress changes are obtained only for the small fault-like structure SD3. This structure is located 300m from the nearest hydraulic fracture stage and only slightly exceeds the level of 0.1 MPa at which stress triggering of earthquakes is considered unlikely. The worst case scenario modelling indicates that the highest DCS is associated with sleeve 47. This is due to sleeve 47 being the final injection point (note; there are only 45 stages permitted, 47 sleeves provides a level of redundancy) in the well and the DCS calculations being modelled from the cumulative impact of all 47 stages. In reality stress build up will be dynamic, with stress redistributing in other areas or released through flow back between fracture stages, and not the static cumulative stress increase as modelled. However using a stepped progressive approach Cuadrilla will monitor any activity on features such as SD3 and alter pumping operation accordingly to reduce the likelihood of stress build up occurring on these features. If these structures are truly faults then potentially they may slip in the course of the fracturing operations. We also conclude these small structures pose a low risk of providing pathways for fluid migration outside of the permitted boundary due to their limited size and constraint as demonstrated by the microseismic data observed so far. The same applies to the small fault-like structures intersected during drilling. In addition to the critical stress modelling, which demonstrated a low risk to fracture or fault growth outside the permitted boundary, a number of mitigation measures will be employed while fracturing operations take place. These mitigation measures are detailed in section s "Permit boundary / Microseismic monitoring”.

l Background Seismicity Results & Interpretation

A baseline of twelve months (Jan 2015 to Dec 2015) monitoring via 7 broadband seismometers has been conducted. No seismicity (events) were detected within the permitted boundary (19 events from 0.7-4.2 M_L were detected outside the permitted boundary with the nearest event at 36 km) and the data was provided to the British Geological Survey (BGS)(2).

In general, noise sources include mainly two types: instrument intrinsic noise and ambient or seismic noise. Seismic noise sources are often located at the surface of the Earth and caused by human-related activities such as traffic, factories, hydraulic treatment related noise, etc. and natural sources like wind, rain, water or waves.

No current mining related noise activities have been identified in proximity to PNR activities, although the Lancashire coal fields and offshore East Irish Sea oil & gas production may provide background seismicity. This will be reported if occurring during the monitoring period. Below 10 Hz there is the Low noise and High noise models derived from broadband seismometers (Abercrombie & Leary, 1993)[16], so expectation is that background seismic noise level will fall between these two bounds. Above 10 Hz there is a fairly steep drop-off in terms of sensitivity of broadband instruments (seismometers) so geophones will likely be more sensitive. The above local noise sources are distinguishable from coherent downhole events with specific move-out. Noise reduction is achieved by applying pre-processing schemes such as predictive and adaptive filtering, stacking, and digital grouping/beamforming. For buried shallow-hole monitoring, noise is highly correlated with the pumping operations. Geophysical processes are able to distinguish coherent downhole events with a specific move-out from other coherent (or not) surface/cultural events.

3.0 Previous & Planned Operations

	Elswick-1	**Preese Hall-1**	**Preston New Road-1z**	**Preston New Road-1z (re-entry)**	**Preston New Road-2**
Well Type	Vertical	Vertical	Horizontal	Horizontal	Horizontal
Fluid Options	Gelled-water with CO_2	Slickwater	Slickwater,	Slickwater, hybrid or gel	Slickwater, hybrid or gel
Sleeves	n/a	n/a	41	41	47
Stages	1	5	17	Up to 45	Up to 45
Hydraulic Fracturing Fluid Volume per Stage	163 m^3 water 24.3 t CO_2	Maximum 2339 m^3	Maximum 466.3 m^3	Up to 765 m3 (Cumulative)	Up to 765 m3
Proppant weight per Stage	58.5 t	Maximum 116.6 t	Maximum 50.8 t	Up to 75 t (Cumulative)	Up to 75 t
Seismic Monitoring		National BGS Network [10]	National & Local BGS Network	National & Local BGS Network	National & Local BGS Network
			Local real-time 8 station array	Local real-time 8 station array	Local real-time 8 station array
			Real-time downhole microseismic monitoring array	Real-time downhole microseismic monitoring array	Real-time downhole microseismic monitoring array
Pre Operational Investigations	2D Seismic Interpretation	2D Seismic Interpretation	3D Seismic Interpretation[11]	3D Seismic Interpretation[11]	3D Seismic Interpretation[11]
			Geomechanical study[3]	Geomechanical study[3]	Geomechanical study[3]
Induced Seismicity	None noted	1.5 & 2.3 (M_L) Induced [10][4]	6 events >= 0.5 (M_L) Induced	n/a	n/a

4.0 Proposed Injection Design & Fracture Modelling

	Including fluid & Sliding sleeve & Coil tubing
Injection / Stage	Up to 765 m^3 (Schedule 3 Table S3.2 EPR/AB3101MW)[5]
Proppant/ Stage	Up to 75 t proppant per stage | 100 mesh, 40/70 Congleton sand and/or 30/50 mesh Chelford sand[6] or similar
Additives	Option list in accordance with (Schedule 1 A5 (EPR/AB3101MW)[5] - Slickwater frac: Polyacrylamide up to 0.05% by volume - Hybrid fluids: Polyacrylamide up to 1% by volume - Gel fluids: Constituents in accordance with Appendix F of Waste Management Plan[19]. The use of these additives may be singular or combined in accordance with operational needs.
Estimated Pumping Pressure / Rate	Surface 51.7 Mpa [7500 psi] - 3.6 m^3/minute
Maximum Pumping Pressure / Rate	Surface 65.5 Mpa [9500 psi] - 6.375 m^3/minute (Schedule 3 Table S3.2 (EPR/AB3101MW)) [5]
Wellbore Deviation Plan / Injection Points	See Appendix 3

m Fracture Modelling

Following completing drilling of PNR2 a static geomodel was constructed, combining seismic interpretation, well picks and azimuthal gamma driven interpretation. This geomodel comprised 12 horizons bisected by major reverse faults, segmenting the model into fault blocks. A Discrete Fracture Network (DFN) was created with 5 fracture sets representing the structures observed in PNR2 by the azimuthal gamma and bedding dip changes. These 5 fracture models were run at sleeve locations; 1, 10, 19, 35 and 47. They were chosen based on their representation of a section of similar geomechanical facies along the lateral and proximity to observed structures. As such they represent the worst case scenario of direct injection into a structure, which could be a sub seismic resolution fault, providing the highest likelihood of creating a pathway for fracturing fluid outside of the permitted boundary.

The model was populated by combining fracture directions and intensity taken from borehole image interpretation in the PNR1 pilot well, and combined with a “Distance to Fault” fracture driver. Geomechanical parameters including static rock moduli, formation pressure, and local tectonic stress field outlined within this document provided boundary condition into this model. They determine the critical well pressures required to initiate hydraulic fractures and they control the fracture growth.

The geomechanical model for the Bowland Shale formation was built by first estimating mechanical properties, pressures, and stress profiles near the pilot hole PNR1, using the wireline logs acquired in that well. The properties were extrapolated along the stratigraphic horizons in the static geomodel. The fracture geometry (hydraulic height, width and length) is controlled by the geomechanical inputs (such as Young’s modulus, minimum stress/stress contrast, Poisson ratio, rock toughness), fluid leak-off and formation parameters (permeability, porosity, reservoir pressure) and imposed conditions such as fluid type, sand concentration and pump rate.

To estimate the magnitude and direction of the in-situ stress field and its variations within the Bowland Shale, a numerical simulation approach was adopted. The results capture the natural stress variations that are associated with the suspected fault zones. Fracture simulation modelling for DFN scenarios was carried out using a Schlumberger proprietary modelling software, called Kinetix®. Fracture models were performed at the maximum allowable injection volume ($765m^3$) at the 5 sleeve locations aforementioned (1, 10, 19, 35 and 47). The Fracture models were performed 3 separate times to provide a sensitivity of fracture growth to the density of natural fractures within the matrix. At all 5 sleeve locations modelled with the 3 sensitivities to natural fracturing not one modelled fracture provided a pathway for fluid migration outside of the permitted boundary. Additionally fluid viscosity was altered within the same model to incorporate the use of hybrids and gels. In all cases the modelled fracture remained within the permitted boundary. Therefore the risk of creating a pathway for fluid migration outside the permitted boundary is considered very low. Additional mitigation measures detailed in section s will provide a real time ability to further reduce the risk of fracturing fluid travelling outside the permitted boundary. Fracture metrics can be found in the table below and graphics in appendix 5.

Proximity of sleeves within the nearest wellbore (PNR1z) is a minimum of 233m at the toe of PNR2, increasing to 292m at the final sleeve of each well. The potential for fracture interaction is deemed low due to the well offset in both depth and latitude and the wells placement within different geological formations with unique geological/geomechanical horizons between the two, including the Upper to Lower Bowland Shales boundary. Therefore effects on the risk of hydraulic fractures propagating outside the permit zone due to these effects is deemed low and will be mitigated through the monitoring proposed in this document.

Any direct wellbore interaction is mitigated by the presence of two barriers in the PNR1z wellbore during stimulation and the continued monitoring of both PNR1z and PNR2 wellbores.

Interference effects of previous injections to microseismic monitoring will be seen through velocity variations. Ongoing recalibration of the velocity model proposed in Section 7.0 Verification Updates will mitigate against any inaccuracies.

Kinetix 3D fracture simulation model of high density DFN based on PNR2 geology

Viscosity	Sleeve	Propped Width (mm)	Avg Fracture Height (m)	Avg Fracture Length (m)
1 Centipoise Slickwater	1	1.6	64	254
	10	2	65	162
	19	1.9	77	138
	35	1.7	73	289
	47	2.9	46	556
30 Centipoise Hybrid	1	0.7	52	681
	10	1.5	26	204
	19	2.9	54	142
	35	0.6	63	991
	47	0.6	42	438
290 Centipoise Gel	1	1	69	583
	10	3.8	49	148
	19	2.0	49	210
	35	0.6	76	643
	47	0.8	48	381

For PNR2, the minimum vertical distance between upper permit red line boundary and wellbore is 200m at the closest point.

5.0 Mitigation Methods and Monitoring

Including Traffic Light System (TLS) & Microseismic & Vibration			
Traffic Light System (TLS)	8 real-time seismometers installed[12]	Combination of broadband seismometers and 4.5 Hz, 3 component geophones. Minimum of 6 required for operational TLS[14]	Detectability during PNR1z operations -0.8 (M_L), P50 average uncertainty, 288 m observed, which confirmed our estimation. Estimated detectability -0.8 (M_L), accuracy 300 m (X,Y) 300 m (Z) at estimated injection depth. Note microseismic array is the primary hypocenter monitoring array, not TLS. Estimate of location accuracy, including parameters, will be made available to the EA on request
TLS Monitoring Duration	Continuous real-time monitored 1 week prior and 2 weeks after final injection operations. The 4 week baseline recorded during initial operations (2018) will be used as the reference period. An additional 4 week baseline monitoring will not be performed due to previous hydraulic fracturing. During operations (24 hours)[12]. Real-time automatic event detection alert (Email) within 60 secs. Manual re-processing (involving downloading data, loading, manually pick and processing) within 20 mins of alert and display online (web portal) (depends on multiple factors including event rate, noise level, event location, magnitude).		
TLS Array Location	Instruments installed in an array from 1.0 km to 3.9 km from the site and have been independently assessed as to quantity, location and redundancy [12].		
TLS Decision Tree	See Appendix 4		
Vibration Monitoring System	Minimum of 4 peak particle velocity (PPV) monitors active in addition to PPV data from 8 TLS stations		
Vibration Monitoring Duration	Monitored before and after operations (2 weeks). During operations (24 hours)		
Vibration Monitoring Decision tree	See Appendix 4		
Operational Boundary	Within the areal extent of the TLS, see appendix 3		

<table>
<tr><th colspan="3">Microseismic Array & Fracture Mapping</th></tr>
<tr>
<td>Real-Time Downhole Microseismic Monitoring Array with downhole recording within 5 minutes and all events displayed for validation. 12 slim hole, 3 component 3 - 200Hz Geophone Accelerometer, (“GAC”)</td>
<td>Estimated detectability based on a simulation model given by the Contractor is given in the HFP, Velocity modelling for this estimate was based on Preese Hall logs tied to PNR1z. Modelled assumptions are;
• P picking error: +- 2 ms
• S picking error: +- 3 ms
• P azimuth error: +- 10 deg
• S azimuth error: +- 10 deg
• Noise Level: 5.7E-9 m/s2
• Qp = Qs = 150
GAC will be verified once in downhole location. Loss in detection efficiency is not expected as long as the number of working shuttles in the array remains between 8 and 12 depending on array aperture. In the event of a loss in detection efficiency backup tools will be used to rectify loss and operations paused until efficiency is restored i.e. greater than or equal to 8 working shuttles. However there are potential scenarios where less than 8 working shuttles can still provide accurate data, however this will be agreed with the EA and can only be demonstrated once the array is downhole.</td>
<td>Estimated detectability -1.8 (M_L), accuracy 25 m (X,Y) 25 m (Z) at the toe of the well.
Detectability during PNR1z pumping -2.1 (M_w) post pumping -2.4 (Mw), P50 average uncertainty, 29 m at the toe of the well, confirming estimation. Updated location accuracy will be provided once the GAC’s are in final downhole position and tests are complete. A report or letter (explains the installation and tool test) will be issued to the Environment Agency within 5 working days of the tests being completed.
Multiple pre-acquisition models were built for microseismic monitoring. Estimation of event detection is described in Raymer & Leslie 2011(15). These utilize Preese Hall well recorded velocity, sonic & density data and consider the planned PNR1z, PNR2 well profiles. The 25 m estimated accuracy is a threshold, rather than a specific value.
Microseismic monitoring will be able to detect fractures within the target reservoir and also into overlying strata. Modelling has been conducted to provide confidence of the detectability within the target formation to the depths of up to 1800m.
With regard to the azimuth errors, these are estimations of the azimuth accuracy for each tool, and not final computed back azimuth accuracies.
Estimate of location accuracy, including parameters, will be made available to the EA on request.</td>
</tr>
</table>

n Assumption Checking

In collaboration with the appointed contractor, Cuadrilla updated the velocity model during the hydraulic fracturing operations at PNR1z in 2018 which will form the basis for the PNR2 velocity model. Cuadrilla will verify the PNR2 velocity model using the furthest available downhole source from the array stations. This verification will be performed to account for the potential repositioning of sondes and the effect of previous injections on the velocity model. See section 7.0 Verification Updates for model updates. If an identifiable seismic event is not recorded from an energy source, other means such as vertical stacking of successive records from repeat firing will be employed until an event is identifiable, or an alternate energy source will be considered. Assessment of the background noise will be performed at the beginning of data acquisition to fine tune the triggers and detection parameters assumed during modelling.

In the event of significant decrease events detection during the job, a re-assessment of the background noise will be performed and a re-assessment of detection sensitivity and accuracy will be carried out.

o Microseismic Duration

Real-time monitoring throughout pumping operations with a minimum of 1 hour after the pumping operation unless agreed otherwise in writing with the EA. Best endeavours to archive (electronically stored for record retention) a continuous downhole microseismic dataset with pick record will be conducted continuously throughout the job until the final fracture treatment and monitoring period as detailed in sections 5.0 table and section s.

p Operational Boundary

Within the areal extent of the TLS as per Appendix 3z, the operational boundary is greater than the red line boundary as outlined within the Permit EPRAB3101MW. The purpose of the operational boundary is to provide a limit of detection for seismic events which can be detected to a high degree of certainty.

q Assurance

Microseismic monitoring will be installed and executed by a competent contractor specialising in microseismic monitoring. The contractor will follow its own quality assurance procedures for calibration and data gathering. If there are gaps within the contractor’s procedure(s) which could cause a risk to compliance they will be updated with a new version and re-briefed to contractor’s staff or a site specific document is developed to comply with the permit and operating technique. A series of energy sources will be utilised to calibrate microseismic equipment. The correct function of an individual sonde and associated orthogonal GAC channels can be verified directly from the acquisition system. The coupling will be verified by a qualitative and quantitative (frequency response) analyses of the signal recorded during the calibration. All effort will be made to avoid placing sondes in areas of known poor coupling through use of CBL logs. The entire tool string can be moved and reanchored if a number of sondes are in poorly coupled areas. It should be noted that there is sufficient redundancy of observations, to proceed with poorly coupled sondes and still achieve the required measurement objectives. Any loss of GAC signal will be reported to contractor and subsequently rectified via their internal procedure as per section 5.0 “Mitigation Methods and Monitoring”. If signals are lost from a sufficient number of stations such that the monitoring array is no longer able to perform as designed, then operations must be paused until real-time signals are re-established.

Contractors equipment will be checked on site before entering the well bore and again once in position using a downhole energy source. The energy source will confirm calibration and effectiveness of GACs. The contractor will conduct the calibration of downhole GACs in accordance with their procedure. Ray tracing is performed to compare the modelled travel time with the measured travel time. Interactive and automated model inversion methods provides a velocity model calibration.

An assessment of the array's effectiveness to monitor hydraulic fracturing operations will be conducted before pumping takes place. Waveforms will be monitored to further verify no tool string movement, which manifest as high amplitude noise across all channels. The waveforms will be used to assure and monitor the array operability. The individual sondes include a high side indicator sensor which measures the inclination and roll to verify non movement of sondes. A data acquisition system provides a series of indicators about the health of each downhole tool. High levels of background noise received downhole will reduce the signal to noise ratio and affect the location accuracy of detected events and detection threshold level. However, multiple standard and proprietary geophysical processes which are used, subject to the specific noise filters, are able to distinguish coherent downhole events with a specific move out from other coherent (or not) surface/cultural events. These standard processes will be utilised in real-time and subsequently proprietary methodologies will be utilised after the events.

Elevated background noise will not lead to false event triggers. In the event of significant decrease of events detection during the pumping operation, a re-assessment of the background noise will be performed and a re-assessment of detection sensitivity will be carried out within the limits of detection.

r Microseismic Monitoring / Induced Seismicity Mitigation

The HFP applies an evolutionary approach, as described in the PNR ES Chapter 12(9), to risk assessment and mitigation (operational mitigation)(9). This stepped progressive approach to hydraulic fracturing will consist of an initial mini-fracture stage and modest initial pumped volumes, building up to a maximum pump volume of 765 m^3 per stage. As this staged pumping process continues, an understanding of the performance of the reservoir during hydraulic fracturing is developed by;

1) Monitoring the extent of fracture growth using a real-time downhole microseismic array. If, during hydraulic fracturing, monitoring data indicates possible fault interactions with a preferential flow pathway or an unexpected seismic response is detected, Cuadrilla, as a prudent operator, will adjust or terminate the pumping of fracturing fluid and the pumping schedule would be modified as necessary.

2) Implementation of the TLS. As long as the induced seismicity is <0.0 M_L (Green level) while pumping, operations will continue. If an induced seismicity event occurs in the range of ≥0 M_L to <0.5 M_L (Amber level) while pumping, the fracture stage can be completed. On completion of the injection the well pressure will be reduced. Pumping may then proceed with caution, possibly at reduced parameters. If an event occurs that is ≥0.5 M_L (Red level) while pumping, the fracture stage will be aborted and the flush and flowback procedure will be initiated. Should seismicity occur at or above the red 0.5 M_L level then a vibration monitoring array will be utilised to assess the impact in accordance with BS7358-2. The measurement recorded by the vibration monitoring array and the TLS will then be used to assess the calibration of the ground motion prediction model(13), shown in Appendix 6, and amendments applied if required.

Cuadrilla is anticipating that the horizontal well bore, or the area intended to be hydraulically stimulated, will encounter a number of small local faults(8). Modelling a conservative assumption (direct injection into a predicted or unpredicted critically stressed fault) and using 2000 m^3 stages the upper bound estimate for maximum magnitude possible would be 3.1 M_L(7), which is considered to be a very low likelihood(9).

If surface vibration occurs in excess of 15 mm/s PPV (as referenced in BS7358-2) due to injection operations, which is assessed to be a very low likelihood, then future injection operations will be altered to mitigate below the PPV 15 mm/s level by adjusting fluid volume, rate, pressure, and or injection point. Where possible, TLS data will be co-processed with any available BGS data, event magnitude determination will be calculated using the BGS methodology. A trailing event with magnitude >0.5 M_L will require a well integrity check be performed and reported in the same manner as those events detected while pumping is taking place.

Fracture stages will be positioned or altered based on the knowledge of any disturbances identified in the microseismic monitoring, drilling and logging observations and from data acquired from previous frac stages, using the stepped progressive approach described in order to avoid direct injection into a significant fault. The plan to place a microseismic array in the build section of the well provides sufficient detectability and location accuracy. The final location will be confirmed to the Environment Agency after installation via an as built drawing.

Utilising the frac sleeves and monitoring in the lateral is not standard operating procedure. Due to the internal profile of the frac sleeve, i.e. not being smooth, pushing the array along the frac sleeves runs the risk of it getting stuck or damaged along the lateral. If at any stage, not just the pumping phase, there is a loss of well integrity after a seismic event which poses a risk of fluid migration to groundwater we will stop activities and take action to maintain integrity of the well and contact the regulators without delay.

s Permit Boundary / Microseismic Monitoring

An evolutionary process as described in the PNR ES Chapter 12[9] will be employed to understand the performance of the reservoir during fracturing. This stepped progressive approach to hydraulic fracturing will consist of an initial mini-fracture stage and modest initial pumped volumes building up to a maximum pump volume of 765 m^3 per stage. As this process continues, an understanding of the performance of the reservoir during hydraulic fracturing is developed by monitoring the extent of fracture growth using a real-time downhole microseismic array.

If, during hydraulic fracturing, microseismic events indicate possible fracture growth with a preferential flow pathway towards the edge of the permitted boundary, the pumping of fracturing fluid would be adjusted or terminated and the injection programme would be adjusted as necessary to prevent future occurrences. Any significant adjustments or terminations to injection programme will be communicated to the Environment Agency. If fracture fluid is interpreted to be outside of the permitted boundary injection will stop after flushing the well. If significant microseismicity continues to occur after the end of injection, then real-time monitoring will continue until it is clear that fractures are not extending beyond the permitted boundary. A period of 24 hours monitoring will be maintained after the last injection stage. Future injection operations will be altered to comply with the permitted boundary by adjusting fluid volume, rate, pressure, and or injection point.

The operational boundary is greater than the red line boundary as outlined within the permit EPRAB3101MW. The purpose of the operational boundary is to provide a limit of detection for seismic events which can be detected to a high degree of certainty. If a single seismic event or a cluster of seismic events occur outside the permit boundary but inside the operational boundary, the following assessment will take place taking into account the spatial and temporal nature of the events:

1. QC of hypocentre events location
2. Event location in correspondence to the frac sleeve;
3. Distance of the event(s) away from the main frac; and
4. Event location uncertainty within the events towards the cluster or event.
5. Report in accordance with condition 4.3.2 and Schedule 5 of the permit.

Any seismic event(s) occurring outside of the operational boundary will be assumed to have a natural provenance except where there is a clear geomechanical link to faults, fractures or seismic event(s) within the operational boundary. The use of microseismic monitoring will track fracture height growth and length to monitor any relationship with seismicity outside the permitted boundary.

Fracture height growth was shown to be impeded in PNR1z operations due to the presence of geomechanical frac barriers related to lithological changes. Fracture height upward in PNR2 will be similarly impeded by the presence of multiple geomechanical barriers known due to the heterolithic fortestratigraphy.

t Groundwater Monitoring

The Waste Management Plan (HSE-Permit-INS-PNR-006) details groundwater monitoring approach and protection measures. Further details have been submitted and approved in PO4 and PO7 which provides groundwater borehole installation and monitoring. The frequency of monitoring is outlined within the Permit EPR/ AB3101MW.

6.0 Reporting

Cuadrilla will document a daily morning report during hydraulic fracture pumping operations only and also report by exception via the TLS report (amber or red during pumping or red event post pumping) as soon as possible to the same regulators as the morning report.

The morning report will be sent to the Oil and Gas Authority, Environment Agency and Health and Safety Executive the following day after the operation. Cuadrilla will make best endeavors to send the report in the morning.

As per environmental permit (AB3101MW), Table S4.1, quarterly reporting of monitoring data, a schematic of microseismic monitoring data will show the location, orientation and extent of induced fractures.

A display, not included in the morning report, will be available to view the day after the relevant stage for 5 working days. The display will contain cumulative post QC microseismic events up to the relevant stage. The display will have 3 graphical orientations (front, side and plan). This will be available for inspection by the regulators. Cuadrilla will provide this display for the following stages: 1, 2, 3, 5, 10, 15, 20, 25, 30, 35, 40 and 45 and the proceeding cumulative data. In the event of a single QC'd microseismic event located outside the permit boundary, the display outlined above will be provided to the Environment Agency regardless of the stage.

Furthermore Cuadrilla will report in a timely manner on the Cuadrilla e-portal the TLS status.

The following tables provides details of each report.

Morning Report	TLS Report	Post Frac Reporting
Stage (consecutive stimulation), sleeve number, volumes, type of fluid, proppant, rate and chemicals pumped. Well integrity status. Induced seismicity of note. Fracture half-length and height relative to the permit boundary. On completion of an initial mini-fracture Cuadrilla will provide an indication of stress magnitude.	Event summary Event classification Event details Hypocentre information Error/ uncertainties Downhole hypocentre information Ground motion and well integrity Injection information Forward injection schedule/ additional mitigation Base and cross sectional map.	Hypocentre location data to be provided upon request to the EA. End of Well Report as per PON9b+B61 Quarterly report as per S4.1 (EPR/AB3101MW) Micro-seismic data and geophysical data will be made available to the EA upon request

u Seismic Level Requiring Integrity Check & Reporting

If at any stage, not just the pumping phase, there is a loss of well integrity after a seismic event which poses a risk of fluid migration to groundwater we will stop activities and take action to maintain integrity of the well and contact the regulators without delay.

7.0 Verification Updates

The verification reports will be provided to the EA, OGA and HSE as required by their regulatory responsibility as soon as reasonably practicable or a minimum 3 weeks before the start of hydraulic fracturing and will continue to be updated during the hydraulic fracturing process.

v Well Observations

At the location of PNR1 pilot hole the stratigraphic sequence went from Permian Collyhurst Sandstone directly into the Carboniferous Upper Bowland Shale. This boundary is at the angular unconformity known as the Variscan unconformity. The absence of Millstone Grit at this location is due to a high angle reverse fault pushing and folding the Upper Bowland higher than the surrounding structure and end Carboniferous erosional surface coming into contact with the Upper Bowland Shale. Subsequently the red line permit boundary has been pushed upwards to approximately 1300/1400 m TVD. Away from the PNR1 pilot location and above the PNR2 well, seismic evidence demonstrates the presence of Millstone Grit and thus does not affect the red line boundary (see Appendix 2). The subsequent observation has not changed the risk assessment or approach to hydraulic fracturing within the boundaries already established in EPR AB3101MW. The observations have been documented with an updated Appendix 2 cross section. The hydraulic fracturing of PNR1z has not changed these observations.

w Microseismic Model Update

Velocity models have been updated with application of data obtained from the already run sonic and density logs and from Vertical Seismic Profile (VSP) data. The operational plan is to use a downhole calibration energy source to update the velocity model. This model will include an estimate of the detectability magnitude at the furthest hydraulic fracture stage from the array. Best endeavours, i.e. moving the energy source as far into the lateral as possible without compromising the well integrity or potential to have equipment stuck downhole, will be made to get actual data to verify the velocity model at the furthest fracture stage from the array prior to hydraulic fracturing commencing.

8.0 Abbreviations

BGS	British Geological Survey
CBL	Cement bond log
DCS	Coulomb stress change
Deg	Degree
DFN	discrete fracture network
HD	high density
EA	Environment Agency
EMW	equivalent mud weight
ES	environmental statement
Ft	feet
HCl	hydrochloric acid
HFP	Hydraulic Fracture Plan
Km	kilometres
Lat	Latitude
Long	Longitude
M	metres
m^3	cubic metres
MD	measured depth
M_L	local magnitude
mm/sec	millimetres per second
MS	Milliseconds
M/S/ 2	Meters per second square
Mpa	megapascals
OGA	Oil and Gas Authority
Mw	Moment Magnitude
PH	Preese Hall
PNR	Preston New Road
Ppg	pounds per gallon
PPV	peak particle velocity
Psi	pounds per square inch
SG	specific gravity
SHmax	maximum horizontal stress
Shmin	minimum horizontal stress
S-P-R	Source pathway receptor
ST	Slip tendency
SV	Vertical stress
T	tonnes
TD	total depth
TLS	traffic light system
TVD	true vertical depth

9.0 References / Related Documents

1: PNR Environmental Statement - Appendix L Fig. 12

2: http://www.bgs.ac.uk/research/groundwater/shaleGas/monitoring/seismicity.html

3: de Pater, H. & Baisch, S. 2011. Geomechanical Study of Bowland Shale Seismicity, Synthesis Report

4: Clarke, H., Eisner, L., Styles, P. and Turner, P. 2014. Felt seismicity associated with shale gas hydraulic fracturing: The first documented example in Europe, Geophysics. Res. Lett., 41, 23, 8308-8314.

5: Preston New Road Exploration Site Permit numbers EPR/AB3101MW

6: PNR Environmental Statement - Appendix B7

7: de Pater, C.J. & Baisch, S., 2011. Geomechanical Study of Bowland Shale Seismicity. Synthesis Report. For Cuadrilla Resources Ltd. 57pp. - Section 6.

8: PNR Environmental Statement - Chapter 12, para156

9: PNR Environmental Statement - Chapter 12, Summary

10: http://earthquakes.bgs.ac.uk/research/earthquake_hazard_shale_gas.html

11: PNR Environmental Statement - Appendix L10.2.2

12: PNR Environmental Statement - Appendix L10.7

13: PNR Environmental Statement - Appendix L8.3

14: PNR Environmental Statement - Appendix L10.8.01

15: D.G.Raymer, H.D.Leslie, 2011. Microseismic Design & Case Studies. SPE, EAGE

16: R. Abercrombie, P Leary. 1993 Source parameters of small earthquakes recorded at 2.5km depth, Cajon Pass, southern California: Implications for earthquake scaling. Geophysics. Res. Lett., 20, 14, 1511-1514

17: PNR Environmental Statement - Chapter 11 Paragraph 245-256, Page 318

18: PNR 1z Hydraulic Fracture Plan

19: PNR Waste Management Plan, HSE- Permit-INS-PNR-006, version 9, January 2019

Appendix 1: Lower Bowland Depth Structure Map

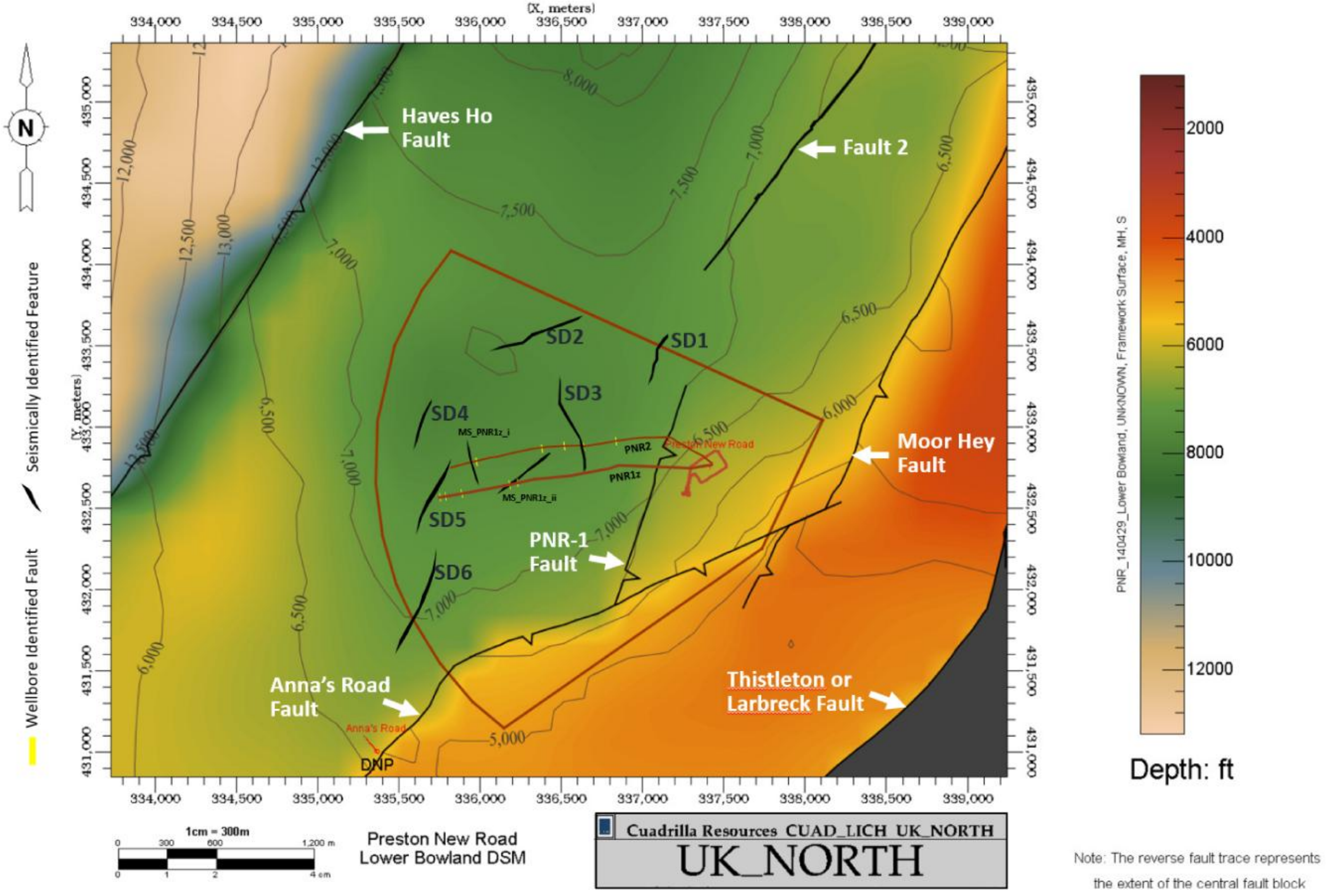

Appendix 2: Sub Surface Information

x Geological Cross Section PNR2

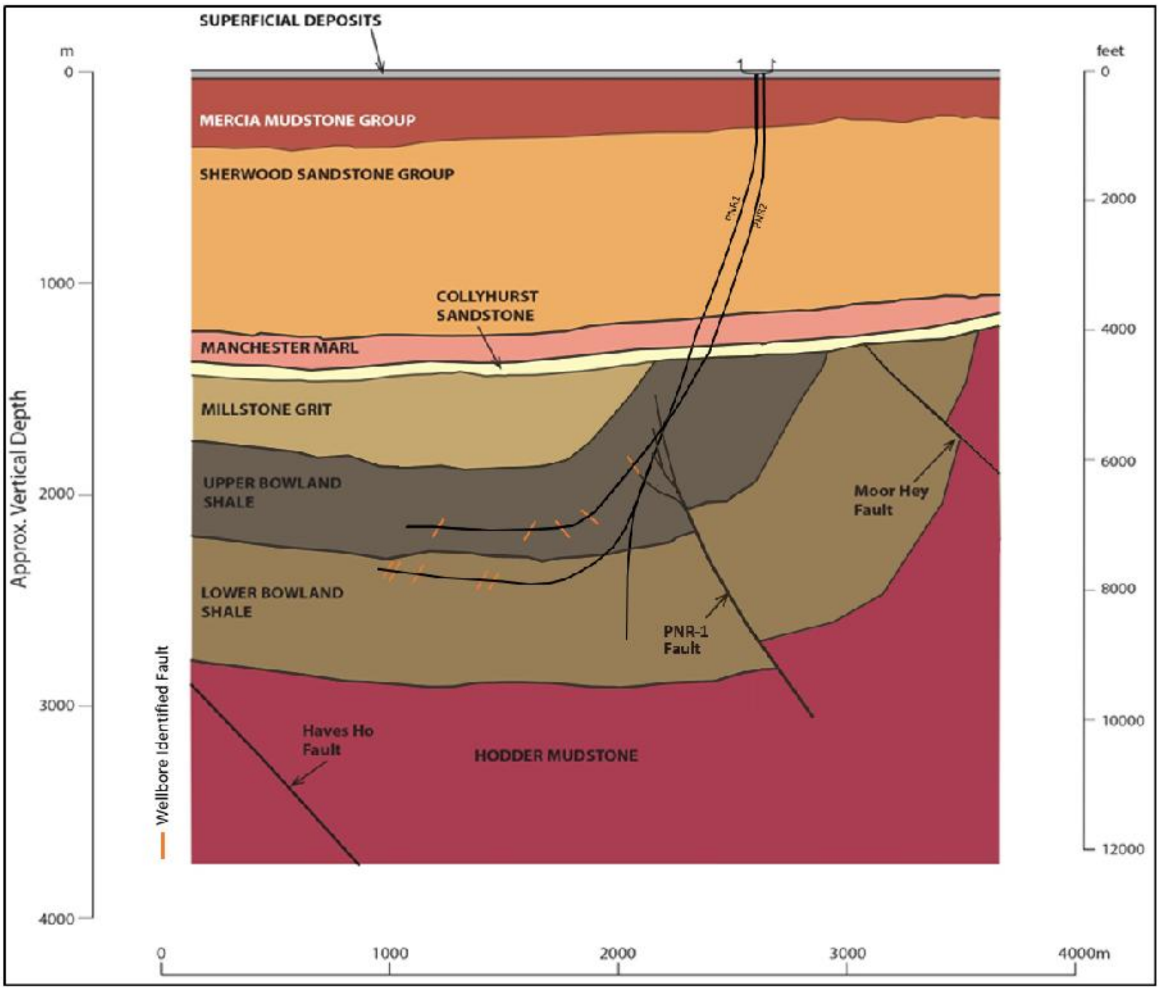

MS_PNR1z_ii feature projected onto cross section following PNR2 well profile

y Seismic Line PNR2

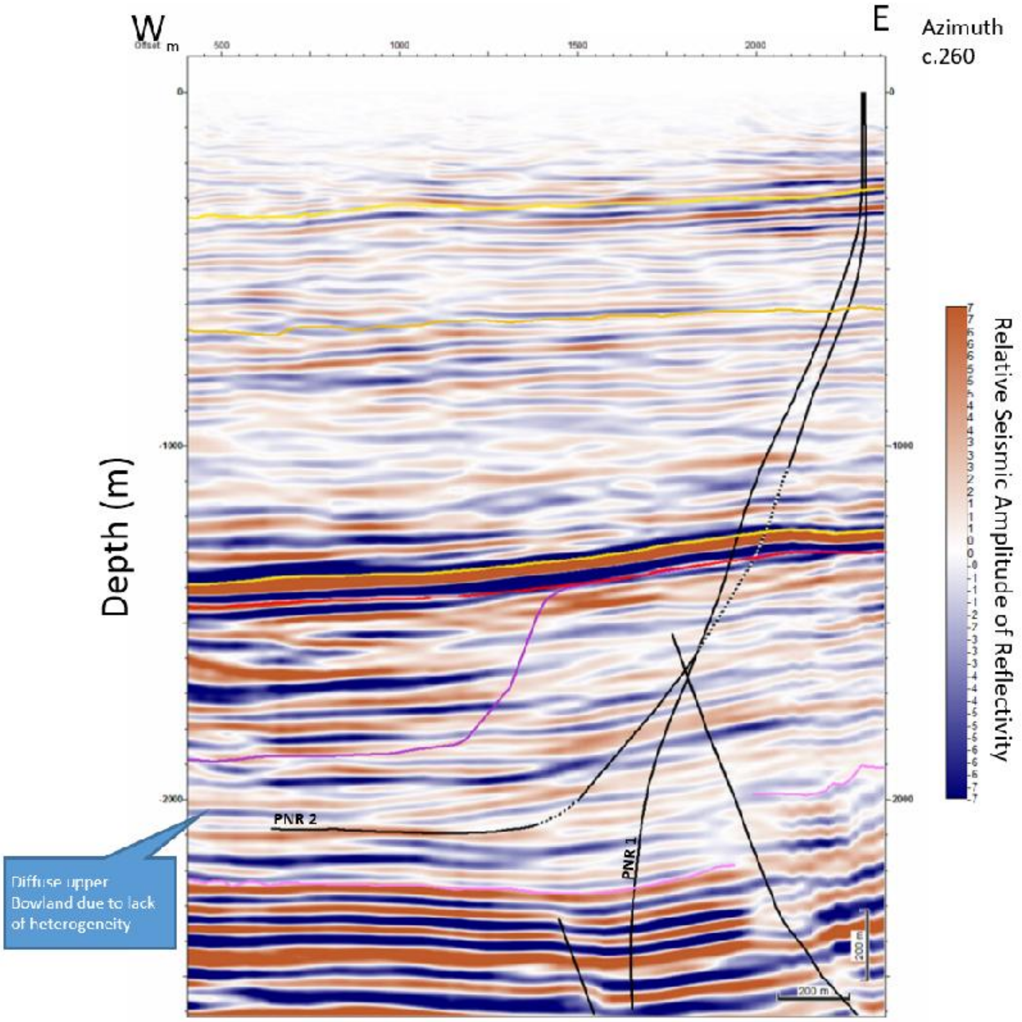

Cuadrilla anticipates that small faults exist at smaller scales than the seismic resolution and cannot rule out the possibility that the seismic discontinuities are potential faults, fracture swarms, depositional features, or seismic artefacts. However these small scale seismic discontinuities will not provide pathways to groundwater receptors because the target formation is isolated from the upper groundwater bearing units by the Manchester Marl Formation. The Manchester Marl Formation underlies the Sherwood Sandstone Group and is a mudstone unit containing primary and diagenetic evaporite minerals. These result in reduced permeability that effectively forms a barrier to upward flow of gases and fluids. For the purpose of this document we have described seismic discontinuities using fault variables, dip, strike, throw.

Appendix 3: Wellbore Profiles

z Wellbore profile, hydraulic injection Locations, indicative microseismic array position

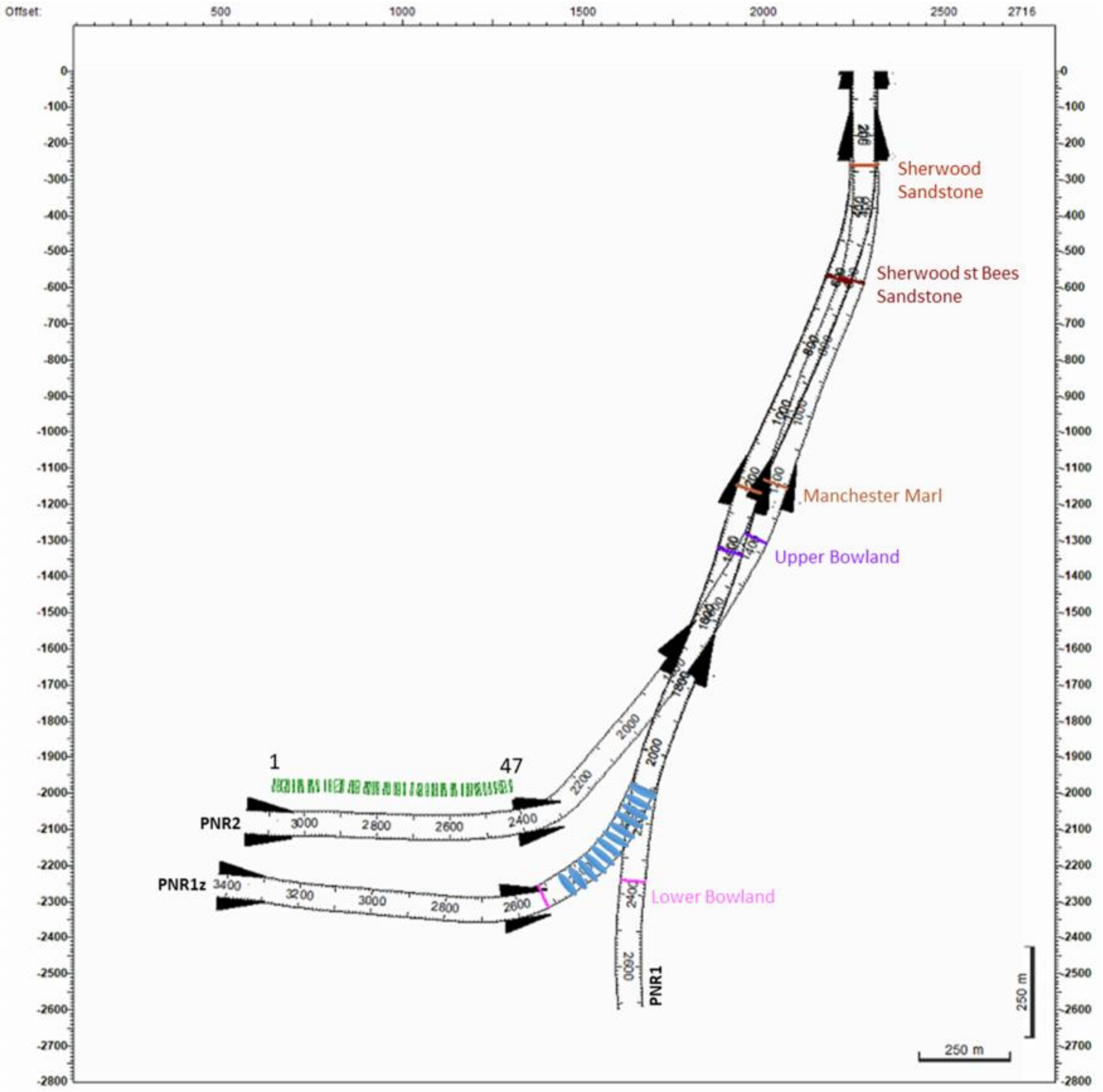

Key

Green: Injection points

Blue: Indicative downhole Microseismic monitoring points

**Wellbore width not to scale*

aa Plan View showing TLS extent of coverage

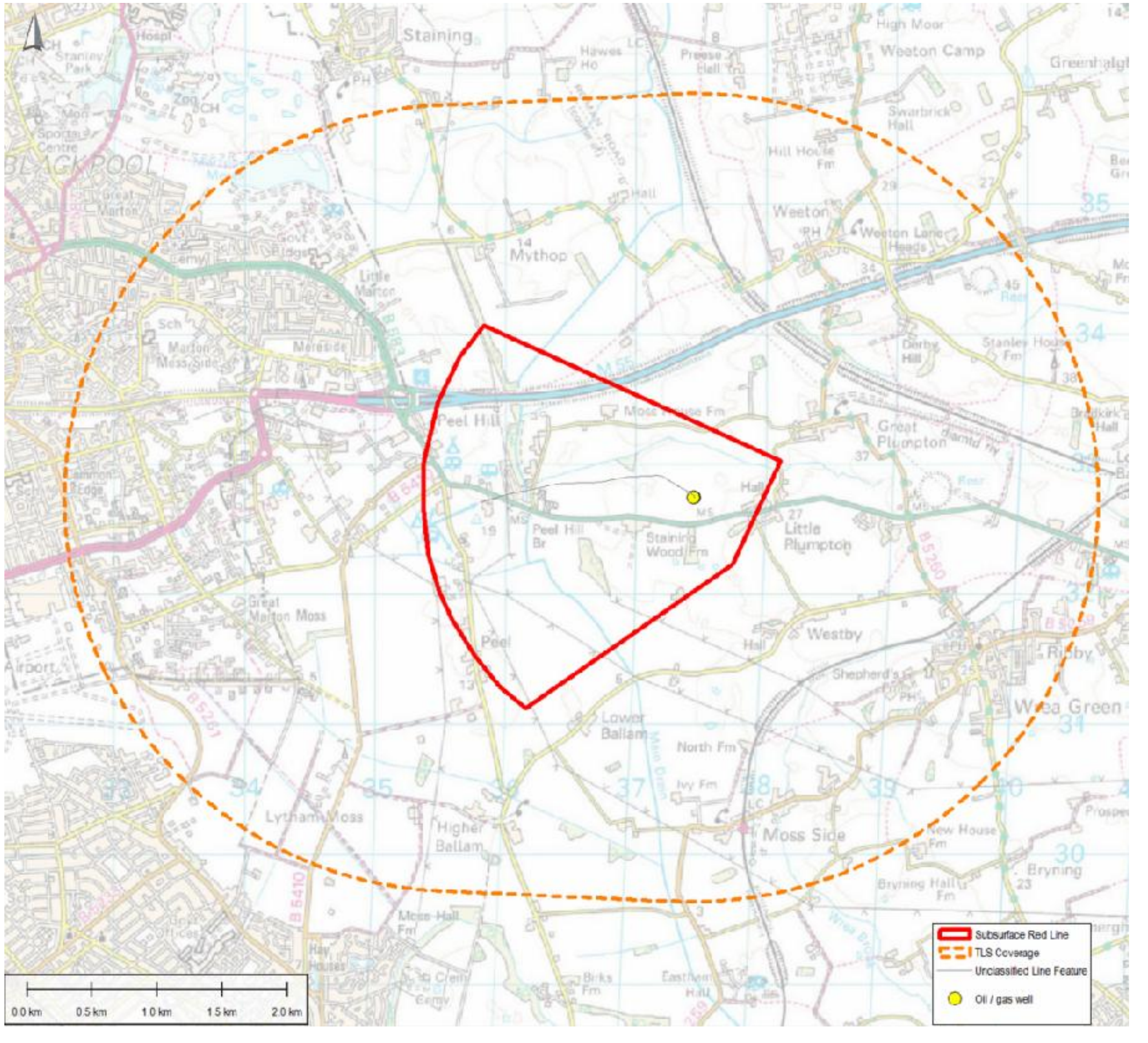

bb 3D representation of EA boundary with wellbore profile

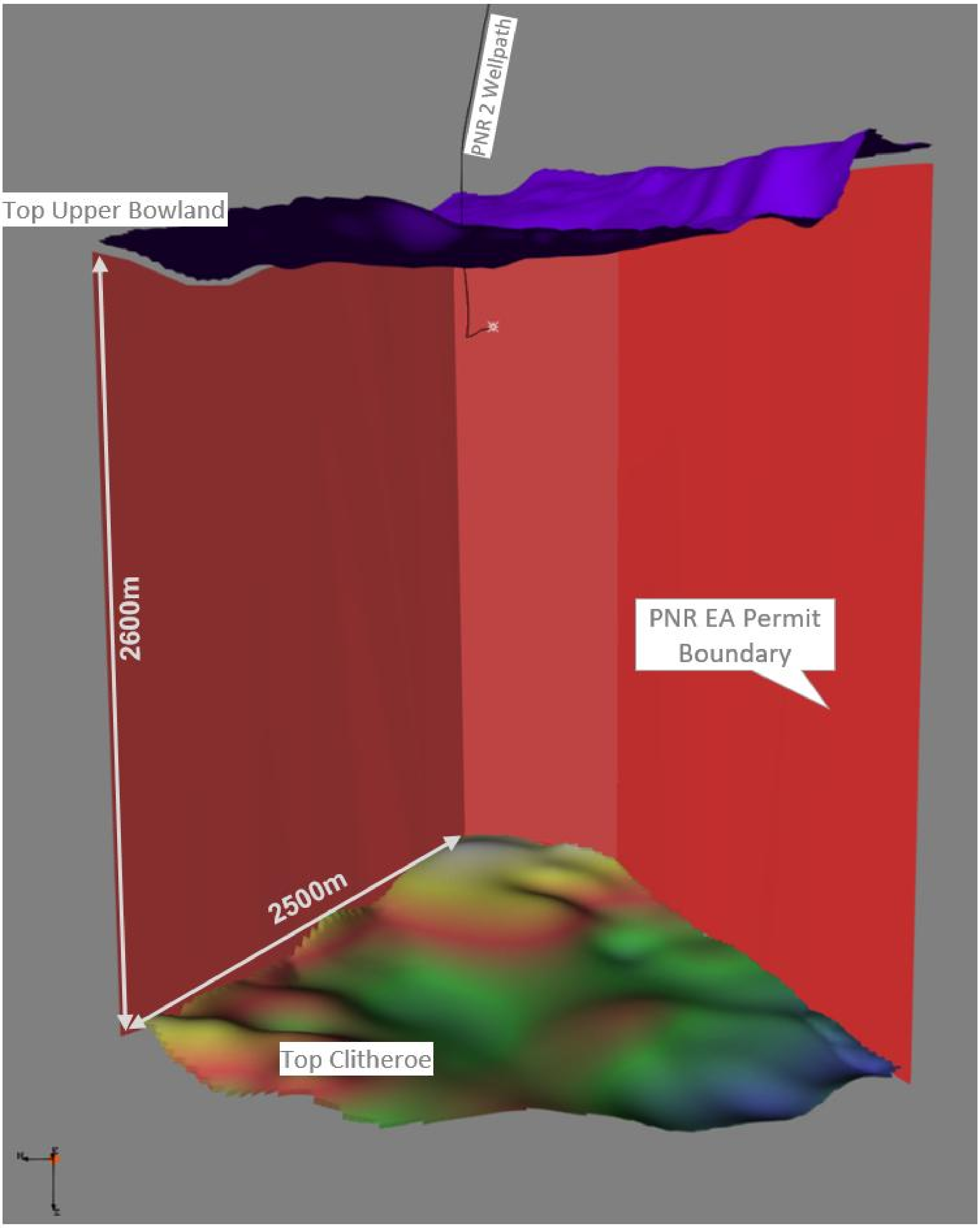

Completions Diagram

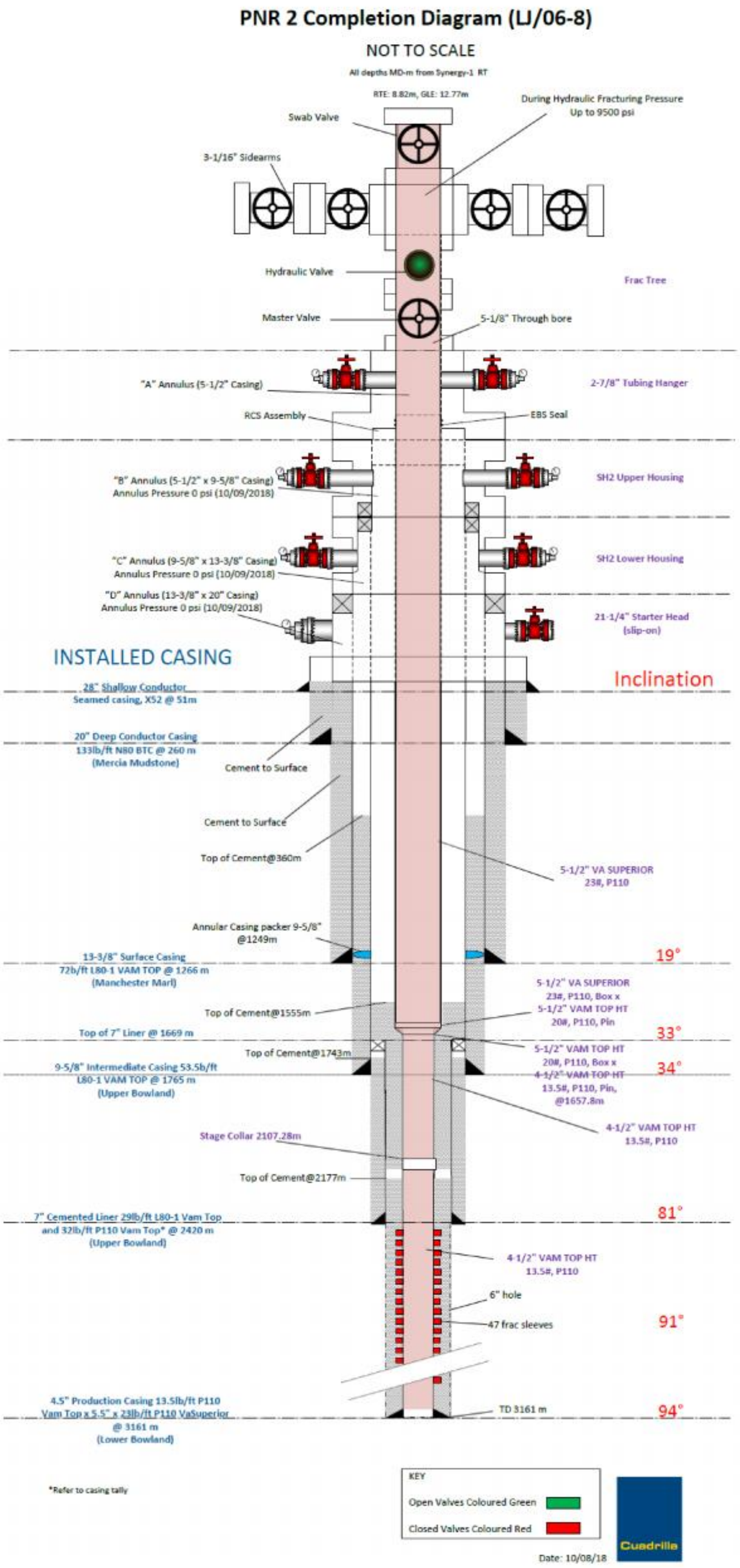

Appendix 4: HVHF Pumping Traffic Light and Surface Vibration System

HVHF Pumping Traffic Light and Surface Vibration System

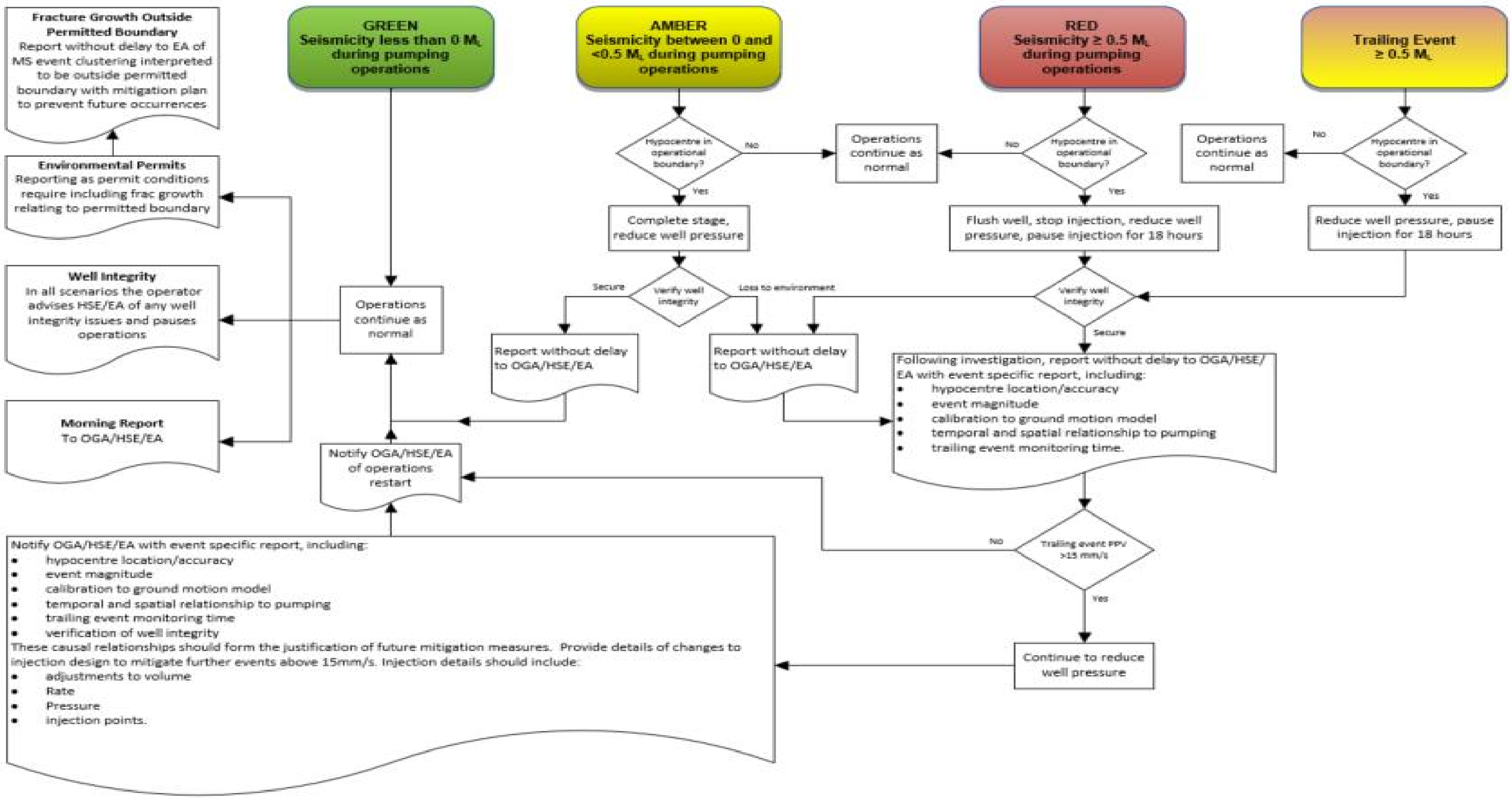

Appendix 5: Fracture Model Graphical Representation

cc 1 centipoise – Slickwater injection

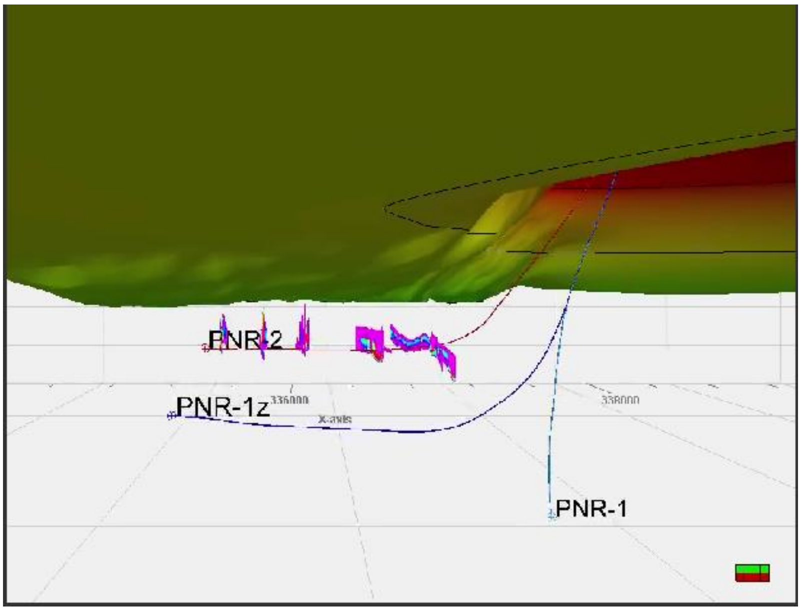

Cross sectional view looking due North across the PNR2 wellbore. The modelled fractures can be seen growing away from the well bore, this represents the complete fracture model not just the average fracture height. The upper limit of the permitted boundary is shown by the contoured horizon, green representing deep moving into red at shallower depths. A grid is provided for scale, each box has a side length of 800m.

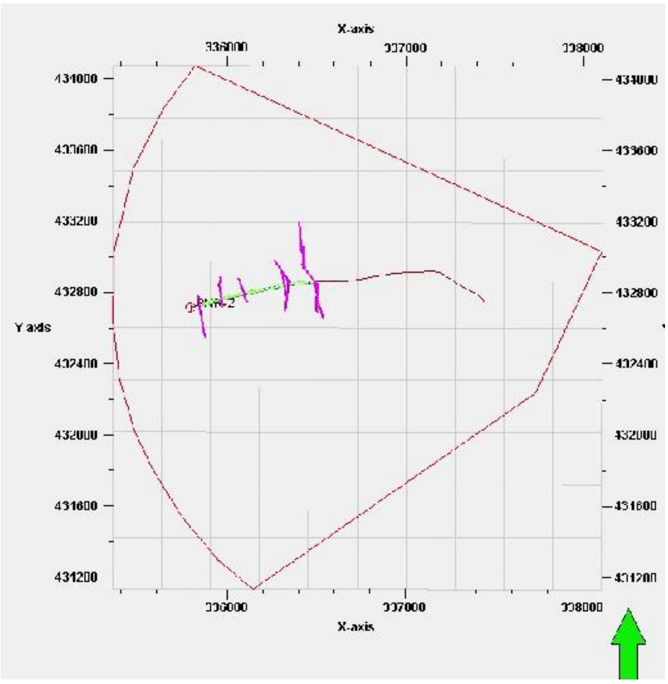

Map view of the permitted boundary, PNR2 wellbore shown in Dark red with Frac Stages shown in Green and the hydraulic fracture models shown in purple.

dd 30 centipoise – "Hybrid" injection

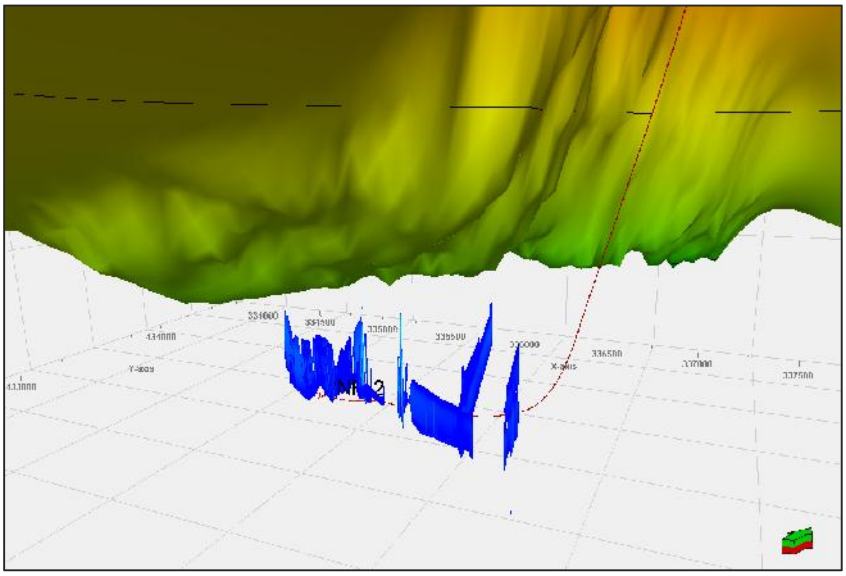

Cross sectional view looking due North across the PNR2 wellbore. The modelled fractures can be seen growing away from the well bore, this represents the complete fracture model not just the average fracture height. The upper limit of the permitted boundary is shown by the contoured horizon, green representing deep moving into yellow/red at shallower depths. A grid is provided for scale, each box has a side length of 500m

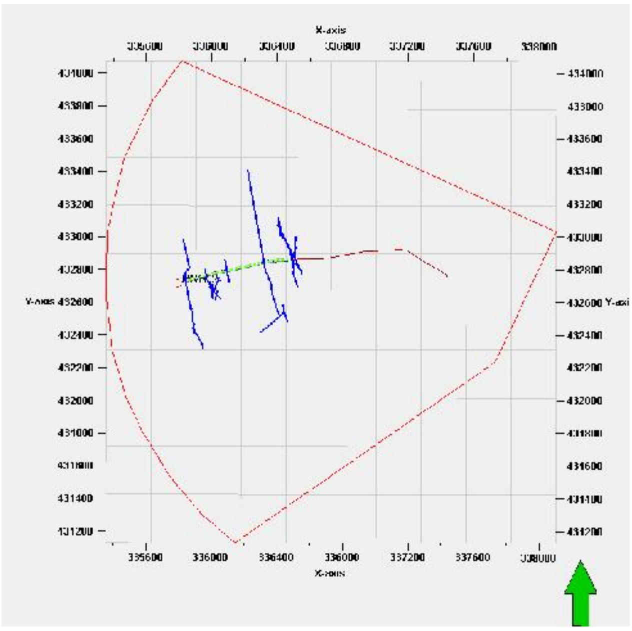

Map view of the permitted boundary, PNR2 wellbore shown in Dark red with Frac Stages shown in Green and the hydraulic fracture models shown in purple.

ee 290 centipoise – Gel Injection

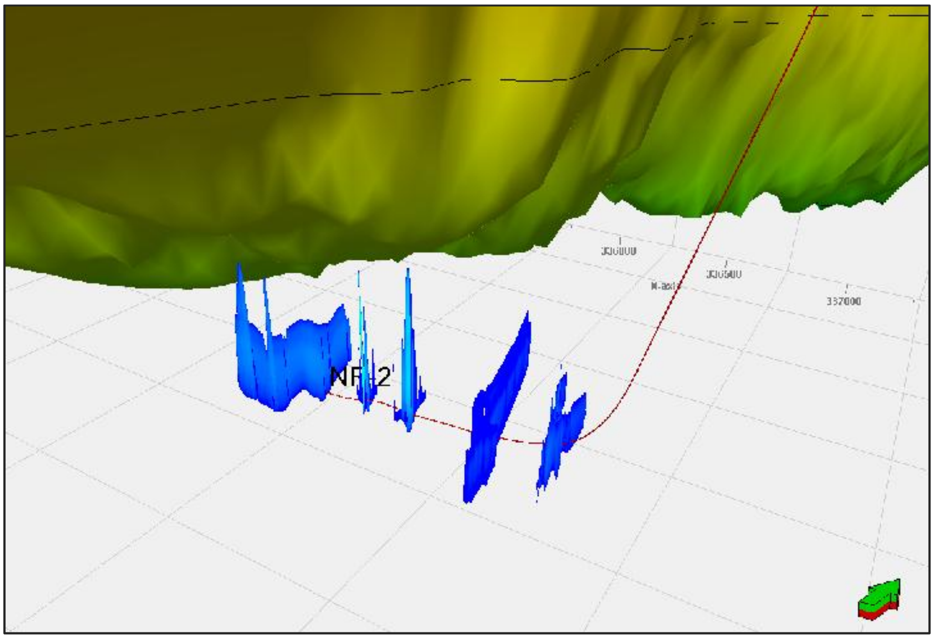

** Clarification note: cross sectional orientation gives a view of fractures into green zone. This is incorrect due to the orientation of the view and not a permit breach. Confirmation is provided in section m, Kinetix table of frac height growth (gel injection).*

Cross sectional view looking due North across the PNR2 wellbore. The modelled fractures can be seen growing away from the well bore, this represents the complete fracture model not just the average fracture height. The upper limit of the permitted boundary is shown by the contoured horizon, green representing deep moving into yellow/red at shallower depths. A grid is provided for scale, each box has a side length of 500m

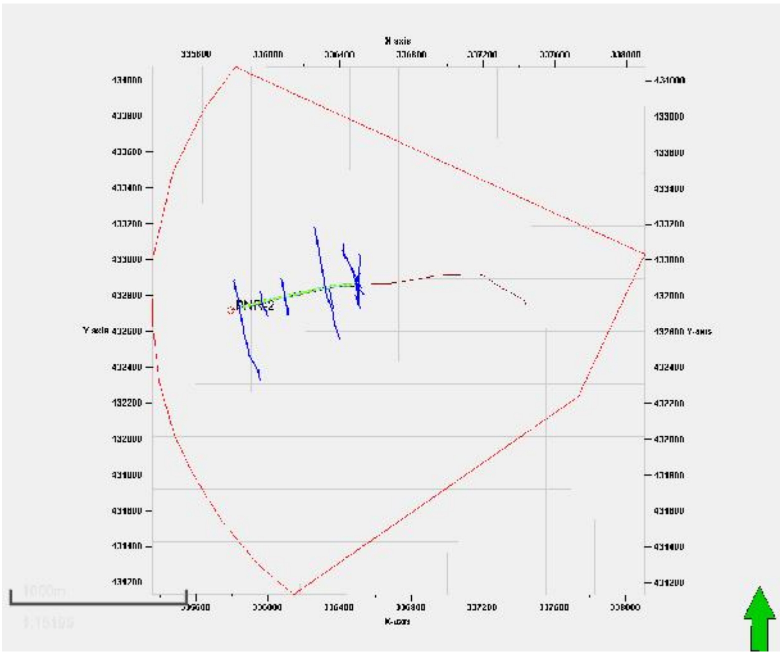

Map view of the permitted boundary, PNR2 wellbore shown in Dark red with Frac Stages shown in Green and the hydraulic fracture models shown in purple.

Appendix 6: Ground Motion Prediction Equation (GMPE)

Overview

Any disturbance caused to people or property by seismic events is as a result of any ground motion induced at surface, rather than directly by the magnitude of the seismic event itself. To understand how these interrelate, the magnitude of a seismic event at its origin within the earth (hypocenter) can be converted into a predicted ground motion at a particular offset, using a Ground Motion Prediction Equation (GMPE). There are a number of models that have been, and continue to be, developed in order to correlate underground seismicity with induced ground motion. Often the models are location specific and rely on historic data from the specific area. A previous study, (Arup, 2014) suggested applying the GMPE by Akkar et al. (2014) to the induced seismicity at Preston New Road.

The various surface monitoring arrays surrounding the PNR operations have provided a very extensive set of Peak Ground Vibration (PGV) data allowing an assessment of predicted vs observed ground vibration in order to refine the GMPE model used. On the basis of this assessment, the Atkinson et al. (2015) model in combination with an appropriate calibration factor, will be used for the PNR site going forward.

Analysis

The majority of modern GMPE's use moment magnitude (Mw) of the seismic event to calculate induced PGV however surface seismic arrays and reported magnitudes are generally recorded and reported as local magnitude (M_L). Therefore, a local M_L-Mw conversion is applied to the M_L recorded by the surface array at Preston New Road before input into the GMPE. This local conversion, shown below, is derived from the Munafo et al, (2016) relationship applied to data acquired at PNR.

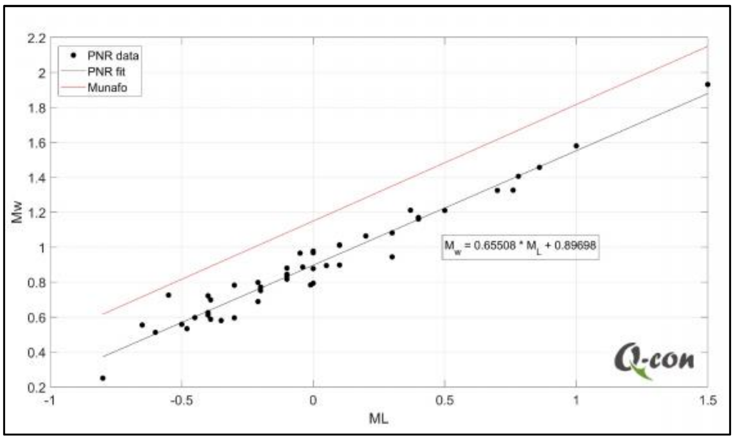

Moment magnitude Mw plotted against local magnitude ML (black dots). Data fit indicates Mw=0.65 ML + 0.9. For comparison, red line denotes relationship found by Munafo et al. (2016).

Vibration observations at PNR, as shown below, suggest Atkinson (2015) in combination with the local M_L to Mw conversion, described above, gives an improvement to the tie between measured (dots) and modelled (lines) ground motion over the previously used Akkar et al. (2014) model. The Atkinson model is therefore the preferred GMPE for the PNR site going forward. This data calibration to appropriate GMPEs will continue as operations progress to improve ground motion predictions.

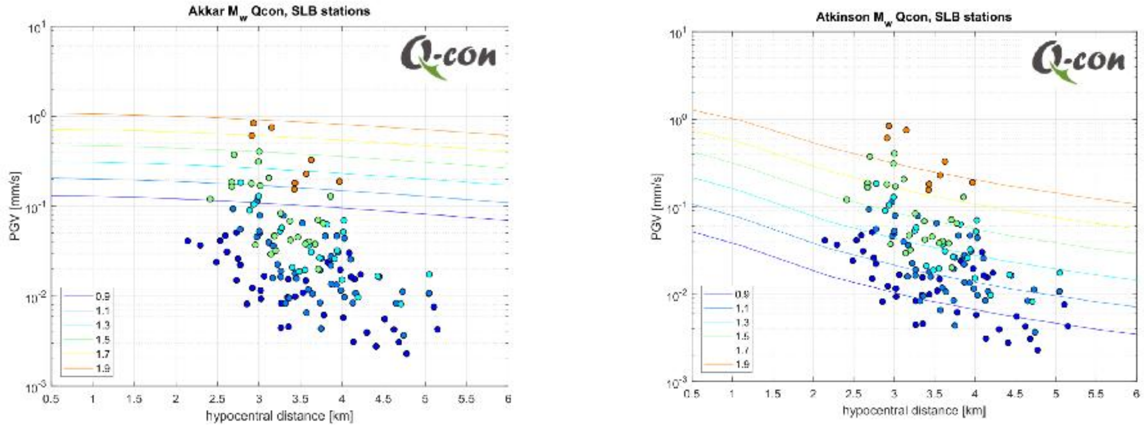

Measured peak ground velocity at SLB stations plotted against Hypocentral distance for the 19 events with ML>0. Magnitudes shown are Mw converted from ML. Coloured dots denote measured values, binned to 0.1 Mw intervals, taken as the maximum of the three-component recordings. Coloured lines denote predicted values according to Akkar et al (2014), left. Atkinson (2015), right. Local magnitude was converted to moment magnitude using the local ML-Mw conversion.

Most modern GMPE's including Atkinson (2015), calculate the geometric mean of the two horizontal components of vibration considered the most likely to cause building damage. However, as human perception, which is specifically considered at PNR, can be sensitive to vertical motion, the maximum of the three components of observed vibration, including vertical motion, is reported and used to tie to an appropriate GMPE. During previous operations the vertical component of vibration was consistently smaller than the two horizontal components. The use of peak component particle velocity, i.e. the maximum of the three components, is in line with current British Standards on vibration. A site specific GMPE cannot be developed without a more complete range of event magnitude observations.

Atkinson et al. (2015) can be expressed as follows:

$$\log_{1} P = -4.151 + 1.762 \cdot M - 0.09509 \cdot M^2 - 1.669 \cdot \log_{1} (R_e) - 0.84 \cdot \log_{1} ({}^{v_{s3}}/_{760})$$

Where:

$$\mathrm{R}_e = \sqrt{(R_{hy}^2 + h_e^2)}$$
$$h_e = M \quad [1, 10^{(-0.2 + 0.1 M)}]$$

Atkinson (2015) calculates the log to base 10 of PGV based on (i) seismic event magnitude (M), (ii) the closest effective distance to the fault rupture plane (Reff) and (iii) a shear velocity term for the top 30 m (V_S30) of soil.

V_S30 is the time averaged shear velocity over the top 30 m (Vs30) also known as site amplification. For the PNR site, a constant V_S30 = 200m/s was conservatively assumed, as proposed by (Arup, 2014), to be consistent with the informed notion that the upper 30m comprises deposits of "dense or medium dense sand and/or gravel or stiff clay; several tens of metres thick"

The chart below illustrates forecast PGV values based on the Atkinson (2015) GMPE fit to observed data for two seismic events, one of magnitude 1.5 Mw and the second of magnitude 3.1 Mw, both conservatively assumed to occur at a depth of 1900m below ground surface.. The chart illustrates the decrease in PGV with increasing epicentral distance i.e. increasing distance from a point at surface directly above the seismic event subsurface location

Seismic events of 1.5 Mw and 3.1 Mw are respectively one and circa three orders of magnitude higher than the Traffic Light System red light level of 0.5. Whilst an event of 3.1 Mw is considered to be the highest possible induced seismic event in the absence of any seismic mitigation, the likelihood of such an event occurring, given the extensive mitigation being applied and detailed within this HFP and the TLS, is considered to be very low.

As GMPEs require Mw rather than M_L and our local conversion is based on a smaller observed range of magnitudes, it is conservatively assumed that M_L = Mw at higher unobserved magnitudes, as suggested by ARUP (2014). The local conversion would give a lower Mw of 2.9 from a 3.1 M_L event. Should events of greater magnitude be observed, a re-evaluation of adequate GMPE and M_L -Mw conversions can be applied to better predict higher magnitude PGV;

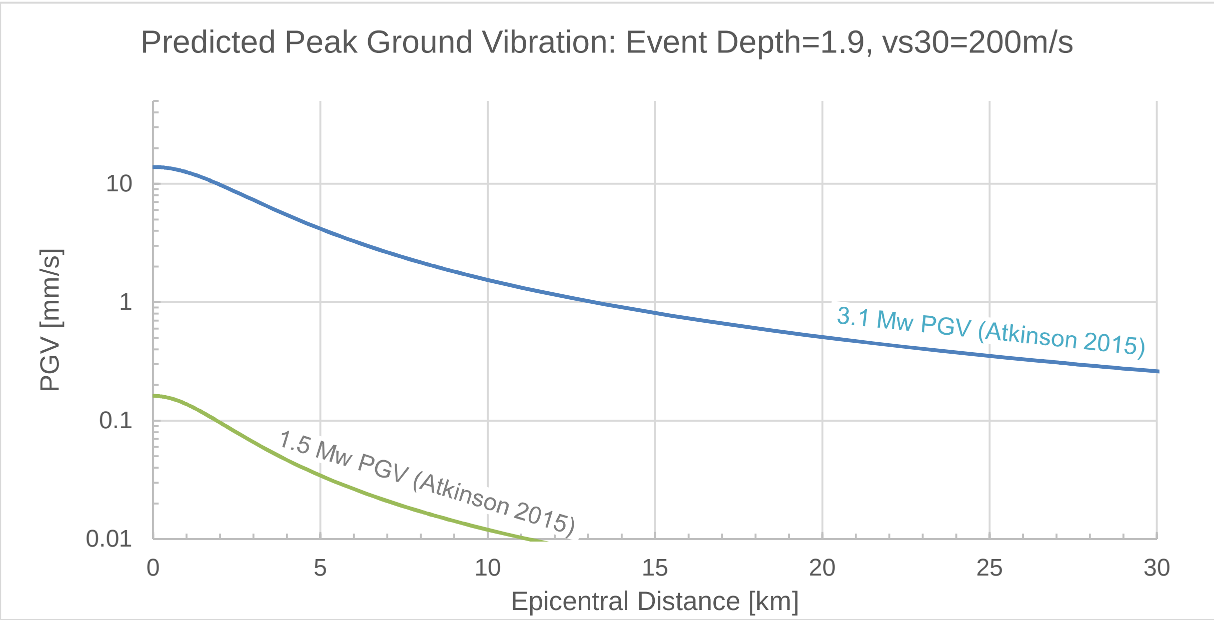

As with any model, there are a range of predicted values around the mean values forecast. When ground motion prediction equations are utilised as part of a seismic hazard assessment, uncertainty exists in two forms, aleatory variability “inherent to the unpredictable nature of future events” and epistemic variability “due to incomplete knowledge and data about the physics of the earthquake process which can theoretically be reduced to zero with sufficient knowledge and observations”.

The Atkinson 2015 equation used to predict peak ground vibration accounts for this uncertainty and has an estimated standard deviation (σ total) of 0.33 around the mean prediction. This means that the range of peak ground motions predicted within minus or plus two standard deviations from the mean for a 1.5Mw seismic event varies from a low of 0.049 mm/s to a high of 0.53 mm/s, both at an epicentral distance of zero. For a 3.1 Mw seismic event, which is assessed as the maximum possible in the absence of any applied seismic mitigation, (i.e. no TLS) the two standard deviation range of predicted ground motions varies from a low of 4.23 mm/s to a high of 45.4 mm/s again measured at zero epicentral distance. Potential for cosmetic damage to buildings from groundbourne vibration is considered in the British Standard (BS 7385-2:1993).

References

Akkar et al, S. S. M. B. J., 2014. Empirical ground-motion models for point and extended-source crustal earthquake scenarios in Europe and the Middle East,. *BULLETIN OF EARTHQUAKE ENGINEERING,* pp. 359-387

Arup, 2014. PNR Environmental Statement - Chapter 12 / Appendix L*,* s.l.: Cuadrilla Resources Ltd

Atkinson, G. M., 2015. Ground-motion prediction equation for small-to-moderate events at short hypocentral distances, with application to induced-seismicity hazards. *Bulletin of the Seismological Society of America,* pp. 981–992

Munafo, I. M. L. &. C. L. 2., 2016. On the Relationship between Mw and ML for Small Earthquakes.. *Bulletin of the Seismological Society of America,* pp. 2402-2408

BSI standards publications

BS 7385-2: 1993, *Guide to damage levels from groundborne vibration*